IEEE Access
Multidisciplinary | Rapid Review | Open Access Journal

Received 11 July 2022, accepted 24 July 2022, date of publication 28 July 2022, date of current version 3 August 2022.

Digital Object Identifier 10.1109/ACCESS.2022.3194652

APPLIED RESEARCH

DeepChannel: Robust Multimodal Outdoor Channel Model Prediction in LTE Networks Using Deep Learning

MOHAMED THARWAT WAHEED[1], YASMINE FAHMY[2], AND AHMED KHATTAB[2], (Senior Member, IEEE)

[1]Department of Technology, Vodafone, 6th of October City 12573, Egypt
[2]Electronics and Communication Department, Cairo University, Giza 12613, Egypt

Corresponding author: Mohamed Tharwat Waheed (mohamed.mohamed-waheed@vodafone.com)

ABSTRACT Accurate channel model predictions are crucial in mobile communication systems to identify the coverage area of cellular base stations. It also allows network operators to optimally choose the locations of the new sites, solve coverage gap problems and optimize the current network parameters. Current prediction models use ray tracing techniques that are too computationally expensive and depend on the 3D maps, which are costly and need to be regularly updated. This paper proposes a multi-modal channel model prediction algorithm using satellite images to extract the environmental features and other numerical features. For an accurate evaluation, experimental measurements in the 2100 MHz band are gathered and combined with 2D maps from two different LTE network areas with varying characteristics to practically reference our results and compare the results with the ray-tracing output. Using the well-known AlexNet architecture as a baseline for our model and introducing new numerical features, we achieve a mean absolute error (MAE) of 2.06 dB and 2.6 root-mean-square error (RMSE) with 4.8 dB enhancement compared to only using numerical features. Using transfer learning, we train the model in area one and test it in another area. We achieve 1.47 dB MAE and 1.99 RMSE with 77.34% reduction in the training time.

INDEX TERMS Channel model prediction, coverage estimation, LTE network, deep learning.

I. INTRODUCTION

Coverage prediction plays a critical role in mobile communication systems to identify the coverage gaps and lousy customer experience locations. Also, mobile operators choose the optimum new base station locations for better investment and customer experience enhancement by proper coverage prediction. With the exponential increase in mobile-connected devices and deployment of 5G networks, especially in the sub 6 GHz and mmWave spectrum for wideband spectrum allocation, more base stations are needed for better mobile network coverage. Also, recently preliminary research started to explore channel models in 6G networks in the mmwave/ THz frequency channel to support further enhanced mobile broadband fuMBB, ultra-massive Machine Type Communication (umMTC) [1]. Accordingly, the need for better coverage prediction /channel model has become essential for mobile operators to identify coverage holes. Inadequate mobile network coverage negatively impacts the Quality of Service (QoS) and capacity provided to mobile customers and devices. Therefore, accurate and efficient models are essential for coverage prediction, overall system optimization, resource allocation, and optimum base station placement. Coverage is the geographical area covered by a service provider's network. The User Equipment (UE) will complete a call using a mobile operator network within this area. Therefore, the threshold of the received signal level by UE to complete a call correctly models the coverage area. The received signal level is measured in Long Term Evolution (LTE) networks through the Reference Signal Received Power (RSRP). The RSRP defines the average power received for the Reference Signal (RS) transmitted

The associate editor coordinating the review of this manuscript and approving it for publication was Yafei Hou.

from a cell in LTE networks. Typically, the UE calculates the RSRP for a specific cell at a given location by averaging the received power of multiple resource elements used to transfer the reference signal within the measured frequency bandwidth. RSRP is measured in decibels to one milliwatt (dBm) [2]. Moreover, RSRP is used as an indicator for cell coverage in LTE networks, which differs from one grid or area to another for several reasons: cell density per area, transmitted cell power, area topology, or cell type (indoor cell or outdoor cell) [3].

Radio propagation models use the environmental characteristics and radio waves propagation to measure the RSRP, defining the coverage area. Radio wave propagation suffers from different factors affecting the RSRP, such as absorption, scattering, reflections, and refractions. Therefore, the radio propagation behavior is different according to area characteristics. For example, in urban and sub-urban areas, scattering, reflections, and refractions have the most contributions to the RSRP. While in rural areas, absorption is the main contributor to the RSRP. The transmitted signal from the transmitter to the UE travels through multipath due to the radio wave propagation. The direct Line of Sight (LoS) is the main component for the received signal, along with delayed versions from the transmitted signal due to multipath fading. Each signal path experiences different attenuation values corresponding to the terrain, buildings characteristics (geometry, heights, construction material,...), and angle of arrival (AoA).

Over the years, many models were developed for coverage prediction and path loss modeling. These models, in general, are categorized into two types: deterministic and stochastic models. Stochastic models result from extensive experimental measurements in different areas jointly with statistical analysis to fit a propagation model in other area characteristics. Therefore, stochastic models are simple and require low computation power but with low accuracy. Different models should be studied to use the nearest one developed in a similar area to achieve a high accuracy. Deterministic models depend on the environmental characteristics such as the operating frequency, types of buildings, accurate geometric information about the obstacles and buildings, and material types for all the subjected areas. Extensive simulations are used in radio wave propagation (ray-tracing) to estimate scattering, refractions, and reflections effects on the transmitted signal, calculate the corresponding RSRP values. Hence, deterministic models require accurate and detailed area characteristics by using updated 3-dimensional (3D) maps from maps providers with high resolution. However, these maps have costly operating expenses (OPEX) that are added to the network optimization requirements and must be updated every six months to capture the environmental changes and enhance the prediction accuracy. Deterministic models employ heavy computational and time-consuming process to estimate the RSRP. Therefore, network operators seek new approaches to estimate and build accurate coverage prediction models. For more detailed information about different stochastic and deterministic models, the reader may refer to [4]–[9]. Field measurements are used to measure the quality of the channel models derived using the deterministic or stochastic models using drive test techniques.

Machine learning-based techniques are alternate and exciting methods to solve coverage prediction and estimate the RSRP values. Machine Learning (ML) has gained tremendous momentum in different domains in the last few years. ML maps an input to an output from an extensive dataset using backpropagation to learn the relationship between the input and output [10]. ML solves complex problems, from self-driving cars to machine translations and Natural Language Processing (NLP). An Artificial Neural Network (ANN) and Convolutional Neural Network (CNN) are ML algorithms that are used separately or jointly to solve these problems. In the case of different data types (numerical, images), multi-modal techniques are used to optimize ANN and CNN algorithms. Supervised, semi-Supervised and unsupervised learning are the categories of ML techniques. In supervised learning, the model learns the relation between the input and the output from labeled data. Semi-supervised learning utilizes a minimum number of labeled data to estimate the relation between the input and the output. On the other hand, unsupervised learning tries to cluster or classify the data from unlabeled samples.

Machine-learning techniques are time-consuming and need heavy computational power in the training phase. However, they exploit parallel processing and using dedicated accelerators Graphical/Tensor Processing Units (GPUs, TPUs) in the training process. On the other hand, the prediction process is fast, efficient, and uses less computation power. Recent works leverage machine learning techniques in RSRP and coverage prediction problems. The following subsection discusses the related work and our main contributions.

A. RELATED WORK

In [11], the authors presented predictions for path loss models in an urban environment using traditional machine leaning techniques such as, support vetctor regression, K-nearest neighbor algorithm and random forest for LTE networks. In [12], the authors provided an algorithm to estimate the channel parameters (precisely, the pass loss exponent and the shadowing standard deviation) using a CNN architecture by utilizing satellite images. In [13], the authors provided a model-aided framework to estimate the RSRP by using a single image with rasterization and a link budget model to enhance the prediction output. In [14], the authors used a U-NET CNN architecture to predict signal strength in different locations using 3D maps of the subject area. The authors of [15] provided different machine learning techniques to predict the path loss in unmanned aerial vehicle UAV. The authors in [16] presented a comparative study of propagation path loss prediction using neural networks and random forests in Narrowband Internet of Things (NB-IoT). In [17], the authors presented a deep learning model to predict the path loss for a wireless communication network by extracting some defined features from satellite images based

on specific types of objects and using Principal Component Analysis (PCA) to generate the low-dimensional environmental features to be used by the deep learning model. In [18], the authors presented a deep learning model to predict the large-scale channel fading in mmWave by designing input features and neural-network architecture to capture topographical information around the base station coverage area using U-Net CNN architecture. In [19], the authors presented a deep learning framework to convert some tabular data to an image and, jointly with a high scale map, extract the high-importance features that impact the path loss hence predicting its values. In [20], the authors presented a model using image segmentation using image processing and image transformation. A fuzzy logic algorithm determines the area's type from five main types then applies one of the known propagation models according to area type. In [21], the authors proposed a model to extract the features from satellite images using PCA then used a FeedForward Neural Network (FFNN) to predict the path loss. The authors of [22] proposed machine learning models based on PCA and FFNN with single and multiple features. The authors in [23] provided a model based on extracting images from satellite maps and aided with a simple propagation model to predict the path loss. In [24] the authors presents an artificial neural network (ANN) based multi-dimensional regression framework for path loss modeling ans studied the impact of using different activation functions. In [25] the authors proposed a machine learning based approach to enhance the output of ray tracing techniques by leveraging a pre-identified set of smart predictors, including transmitter parameters and the physical and geometric characteristics of the propagation environment. In [26] the authors presented explainable deep leaning based path loss prediction from path profiles in urban environments using 5G network simulation data. However, most of the previous works have the following limitations and concerns regarding their practical implementation and accepted accuracy from the service provider's point of view:

1) Most of the current work uses ray tracing as a reference, which is inaccurate and not practical. Depending only on the ray tracing for comparison is not an accurate measure of the accepted coverage prediction accuracy, especially for investment allocation [13], [27].
2) The models that use the satellite map can not capture all the environmental features without supporting handcrafted features. Most of the current work uses a high zoom level of a satellite map, which can not accurately capture the topographical characteristics of the area [12], [28].
3) Finally, to the best of our knowledge, there is no prior work with extensive drive test data in a large scale area with many base stations that can be used as the reference in the comparison to identify practical results that will impact service provider's plans efficiently.

The main contributions of our work are summarized below:

TABLE 1. Table of notations.

Symbol	Description
d	Distance between transmitter and receiver.
G_t	Transmitter antenna gain.
G_r	Receiver antenna gain.
f_c	The operating frequency.
$A(f,d)$	The median attenuation as a function of distance and operating frequency.
h_t	Effective antenna height at the transmitter.
h_r	Effective antenna height at the receiver.
$a(h_{re})$	Correction factor for receiver antenna height.
C_m	Environmental characteristics factor.
$\alpha(.)$	Non Linear function.
X_0	Shadowing factor.

1) We propose new features used in our model by creating new handcrafted features from expert/practical point of view from the collected dataset.
2) We propose DeepChannel a multi-modal framework for outdoor channel model estimation based on numerical features and environmental features extracted from satellite maps based on the well-known architecture AlexNet.
3) DeepChannel presents a new and high accurate model to predict coverage map based on historical drive test data which help minimizing the drive test cost.
4) We compare our results with practical measurements LTE dataset in 2100 *MHz* Band collected from two major cities in Egypt (Cairo and Giza) and computerized applications based on ray tracing. We compare our results with other state-of-the-art systems.
5) We use transfer learning between the two datasets using a pre-trained model in one dataset to the other dataset.

The rest of the paper is organized as follows: Section II presents the Channel model prediction model. Section III presents the DeepChannel system model. We then discuss the system performance, comparison, and evaluation in Section V. Finally, Section VI concludes the paper.

Notation: throughout the paper, we use the following acronyms as shown in Table 1.

II. CHANNEL MODEL PREDICTION

Estimating the RSRP value is equivalent to calculating the Path Loss (PL) between the transmitter and the receiver, i.e., figuring out the deterioration in the transmitted power at the receiver.

Using simple curve fitting techniques, the Okumura *et al.* [29] model was developed based on

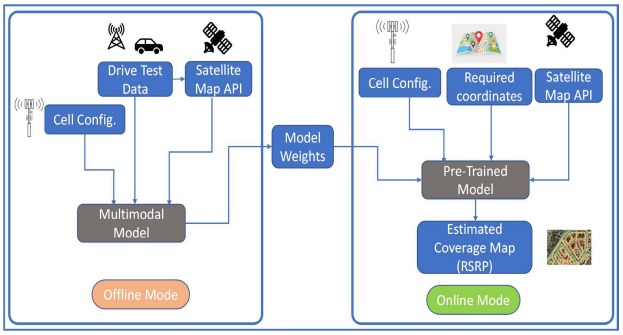

FIGURE 1. System model.

measurement in Tokyo and Japan as shown in equation (1)

$$PL_{median} = \text{FSPL} + A(f, d) - G(h_t) - G_r - G_{Area} \quad (1)$$

where PL_{median} is the median value of the PL, $A(f, d)$ is the median attenuation as a function of distance and the operating frequency, $G(\cdot)$ is the antenna gain, h_t, h_r is the effective antenna height at the transmitter and receiver, and G_{Area} is the gain/attenuation due to the type of the terrain in the operating area. The Hata-Okumura model [30] extends the Okumura model by adding more parameters to fit different terrain types accurately. Reflections, diffraction, and scattering are the main propagation loss for this model. The most common form of this model is defined by equation (2)

$$PL_{urban} = 69.55 + 26\log(f_c) - 13.82\log(h_{te}) - a(h_{re}) + (44.9 - 6.55\log(h_t))\log(d) + C_m \quad (2)$$

where f_c is the operating frequency in MHz, d is the distance between transmitter and receiver in kilometer, h_{te}, h_{re} is the effective heights of the transmitter and receiver, and C_m is a factor dependent on the area and environmental characteristics. $a(h_{re})$ is the correction factor for receiver antenna heights, and it has different values according to the area and environmental characteristics. In the case of small to medium sized cities, equation (3) represent the value of $a(h_{re})$ and C_m

$$a(h_{re}) = (1.1\log(f_c) - 0.7)h_{re} - (1.56\log(f_c) - 0.8), \quad C_m = 0 \quad (3)$$

Similar models were developed based on this analogy trying to figure out propagation models for different environmental areas [31]–[38], hence, calculate the RSRP in different areas. As a generalization for the calculation of the path loss model, we can model the PL as shown by equation (4)

$$PL(d) = \alpha(f_c, h_t, h_r) + \lambda\log(d) + X_0 \quad (4)$$

where $\alpha(f_c, h_t, h_r)$ is a non linear function in the operating frequency, transmitter height, receiver height and area environmental characteristics. λ is a deterministic factor and function in receiver antenna height. Shadowing is the random variations of the received signal (RSRP) around its mean value at a given location. These variations are due to objects and obstacles in the radio path, i.e., shadowing is a measure of the variability in the received signal. X_0 in equation (4) represents the shadowing factor that can be modeled as a Gaussian distribution with zero mean and σ standard deviation [39].

Equation (4) represents a general function that all stochastic models try to figure out its optimum parameters to fit in different areas. This is a nonlinear equation and using basic and traditional curve fitting techniques gives a low accuracy model. Supervised machine learning can be adopted to learn this nonlinear function from the output and a set of input features [10] using labeled data. Neural and Deep Neural Networks (DNN) are a subset of the machine learning discipline and have proven to be a state-of-the-art technique to map non-linear functions from a set of labeled data. Neural network main components are neurons, layers, and activation functions. Each layer of the network consists of multiple neurons, each of which has an output that is a nonlinear function of a weighted sum of the neurons of its previous layer. Hence, the output of the overall neural network is a multi-layer nonlinear transformation to the set of input features. The reader can refer to [40], [41] for more information about neural networks. Accordingly, we can use neural network to learn the optimum parameters of the channel model represented by equation (4). The convolution operation [42] proved to be an efficient way to extract features from images. That was the introduction of a convolutional neural network in machine learning and was the main reason for the significant advancements in extracting features from the images. The reader can refer to [43]–[45] for more details about ConvNet.

As the RSRP values are continuous values, we have two methods for the prediction, either as a classification problem by splitting the values into discrete intervals or as a regression problem [46]. We choose the regression method for accurate and precise predictions. In the next section, we will discuss the proposed system model and how we utilize neural and convolutional networks in our work to predict the nonlinear channel model.

III. SYSTEM MODEL

This section introduces the structure and main blocks of the DeepChannel framework. As depicted in Figure 1, the DeepChannel framework has two modes of operation: an offline mode for training the model and an online mode for estimating the RSRP, and hence, the coverage map in the needed area using the pre-trained model.

A. OFFLINE MODE

In offline mode, we train the model after collecting drive test field measurements, followed by satellite maps Application Programmable Interface (API), cell configuration, and a multi-modal model.

1) DRIVE TEST DATA

Drive tests is one of the main sources to collect measurements data from the field. Such measurements are usually carried out to be used as a primary indication of the coverage and

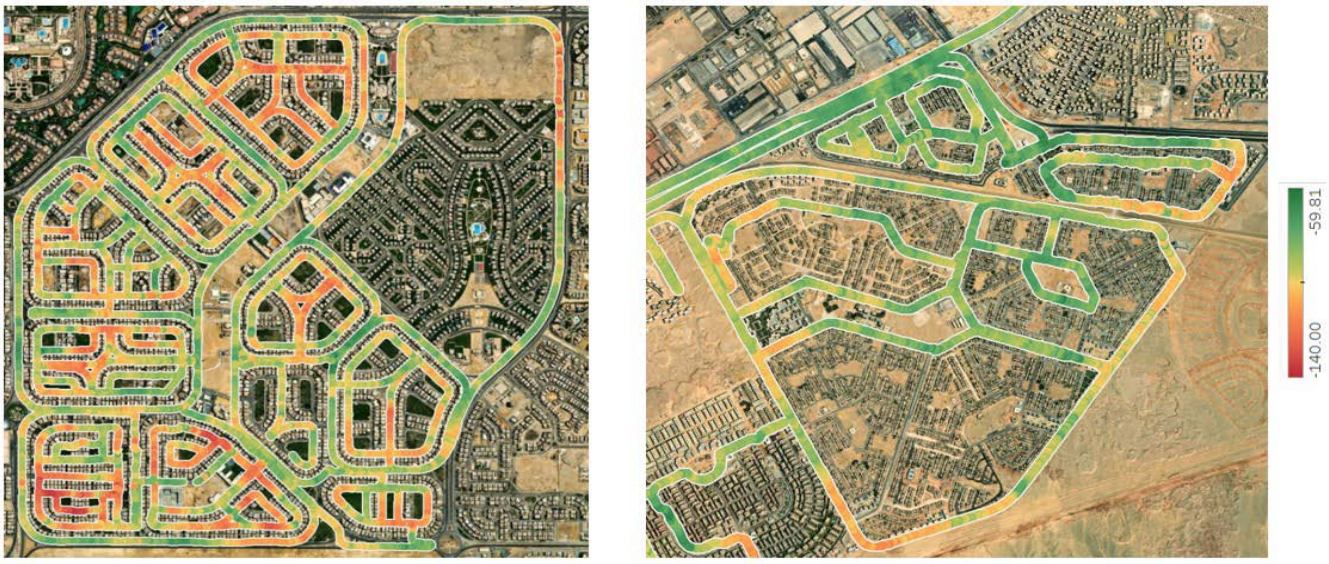

FIGURE 2. Dataset points with range of RSRP value.

performance Key Performance Indicators (KPIs). The main reasons for drive tests are: (1) Coverage optimization based on field measurements enhances the coverage map built from deterministic or stochastic models discussed in Section I; (2) It enables mobility optimization to detect handover failures; (3) Capacity optimization, using drive tests measurements, allows the operators to detect low throughput areas and through correlation with the coverage map it enables detecting the coverage holes and gaps that impact the capacity. Drive tests are usually carried out on a regular basis to detect any coverage or network issues and in many cases after any optimization action taken by the service provider engineering team such as frequency shuffling or re-farming. Drive test is a cost and human efforts process; techniques are required to minimize drive test measurements to save service providers OPEX cost [47]. Data is collected through intensive drive tests in a suburban area using the TEMS solution [48], an autonomous solution that uses smartphones to test data and voice services. Data logs are uploaded or saved periodically for further post-analysis. The used testing unit is a commercial smartphone to simulate a real customer's experience. In our model, we collect the log files through Samsung Galaxy Note8. Two datasets are collected in Cairo and Giza governorates with different area characteristics. Figure 2 shows the collected data with a color legend representing the range of RSRP values. The car's speed was an average road speed of 40 KM/h, sampling interval of 24 $msec$, and the mobile was locked in 4G network using the 2100 MHz B1 band, with carrier bandwidth of 15 MHz. We have different messages exchanged between the UE and the base station. We select the readings for downlink messages. We use a built-in GPS module for accurate coordinates synchronization. The Cairo area dataset spans 8 km^2 with a 24 km driving distance covered by 28 different physical cell identifiers (PCI) which is an identification of a cell in the physical layer. The Giza dataset spans 31 km^2, with a 46 km^2 driving distance covered by another 24 PCIs.

2) SATELLITE MAPS API

Satellite maps have been significantly improved and are now available at a low cost from different providers. The improvement includes various maps with varying zoom levels to capture different types of objects and even street-level details. Also, map providers now support on-the-shelf APIs to facilitate the integration with other systems with different categories. In our proposed work, we use Google Cloud Platform (GCP) [49], a suite of cloud computing services offered by Google. In the satellite maps (API), we combine the collected data with the online satellite map provider to download the satellite image corresponding to a specific location. We utilize the static maps API to download satellite images in all geographical locations where we collected the drive test data. The center of the image corresponds to each point in the drive test data. We use zoom level 19 and image size 640 $\times$ 640, which gives 0.298 $m/pixel$ resolution to capture all environmental details. Figure 3 shows samples of the output of the satellite Maps API for different areas. According to Figure 3, we are able to capture different objects like buildings, roads, trees, and swimming pools (water objects).

3) CELL CONFIGURATION

In the third module, cell-specific parameters and configuration (operating frequency, transmitted power, antenna

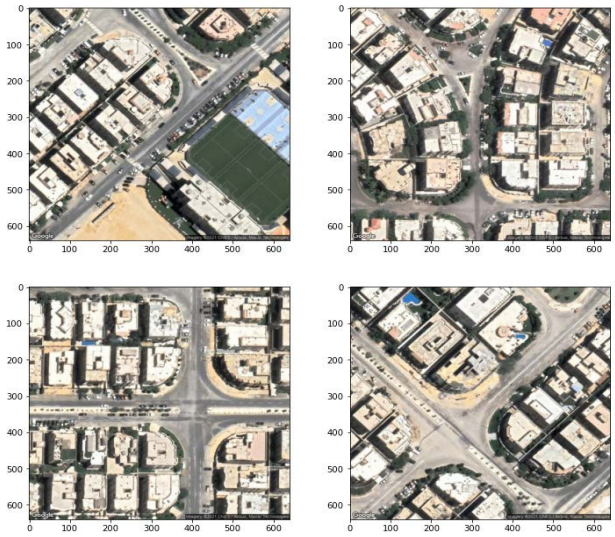

FIGURE 3. Different samples for satellite map API.

heights,...) and the geographical locations of the existing base stations. This data is in the planning tool that the service providers' engineers use to plan and optimize the network. Planning includes the optimal allocation for the new needed base station to achieve specific coverage and customer experience requirements. At the same time, optimizations aim to find the optimum parameters to operate the network efficiently for the same coverage and customer experience requirements. These data are collected with post-processing to fit in the multi-modal model and accurately calculate the hand-crafted features.

4) MULTI-MODAL MODEL

In this section, we present the DeepChannel model starting with the feature engineering module and the AlexNet followed by the multi-modal fusion. Figure 4 presents the detailed blocks of the model, in the next subsections we will explain each block in detail.

a: MULTI-MODAL NEURAL NETWORK

Typical neural networks are used to solve supervised and unsupervised problems for single modalities, i.e., structured numerical features. Typical ConvNet are also used to solve single modalities, i.e., images/videos [50]. While multi-modal networks are used to combine features from different modalities, i.e., combine features from structured numerical features and unstructured features from images resulting in cross-modality feature learning. Different combinations techniques are used to fuse the results of both networks by flattening the output of ConvNet and concatenating or summing the output. Multi-modal techniques are well known in computer vision for fusing multiple sources of information/features. We have three main questions that need to be addressed in multi-modal networks. The first question is what features to fuse, and feature engineering methodologies play a prominent role in answering this question. The second question is how to fuse these features related to different modalities and techniques used, such as addition or average mean, concatenation, ensemble, or a mixture of experts. The reader may refer to [51]–[53] for detailed information about how to fuse different modalities. The last question is when to fuse. Also, we have different strategies for fusion location. We have early, middle, or late fusion depending on the location of the fusion layer in the network structure.

b: FEATURE ENGINEERING

The first block is feature engineering. Feature engineering in machine learning selects the essential features that impact the output [54]. Feature engineering can be categorized into two main types. The first is handcrafted features that use domain knowledge experience to define and extract the needed features. The second is the self-learned features that can be learned and extracted automatically using a machine learning algorithm. In our model, we use a mix between the two types as follows:

1) Handcrafted features:
   a) The distance between the transmitter and receiver is a critical feature in path loss model calculations as discussed in Section II. Using Equation (10) to calculate the distance between the serving transmitter and the UE point $\mathcal{D}$.
   b) Geographical coordinates (Latitude and longitude) for the receiver are used as landmark features for the location $\mathcal{LAT}$, $\mathcal{LONG}$.
   c) Adding a simple path loss model as a feature to aid and guide the model in the right and accurate direction of convergence, we use the Hata-Okumara model defined by Equation (2), PL_{urban}.
   d) Bearing angle between the transmitter and receiver to identify the azimuth direction of the receiver toward the transmitter. Assume that we need to get the bearing between two points $(Lat1, Long1)$ and $(Lat2, Long2)$, we use equations (5),(6),(7), as (8) to get the bearing angle as follows:

$$\Delta long = (Long2 - Long1) \tag{5}$$

$$y = \sin(\Delta long) \cdot \cos(Lat2) \tag{6}$$

$$x = \cos(Lat1) \cdot \sin(Lat2) - \sin(Lat1) \cdot \cos(Lat2) \cdot \cos(\Delta long) \tag{7}$$

$$bearing = \tan^{-1}(x, y) \tag{8}$$

2) Self-learned features: From Equation (1),(2),(3), its clear that the major contributor to the path loss model is the area characteristic that dominates the impact on the RSRP value. Accordingly, capturing the geo-statistics information is a significant factor in the path loss model. In our proposed model, we are using satellite images to extract the geo-statistics information of the environment. Using a Satellite map, we may consider

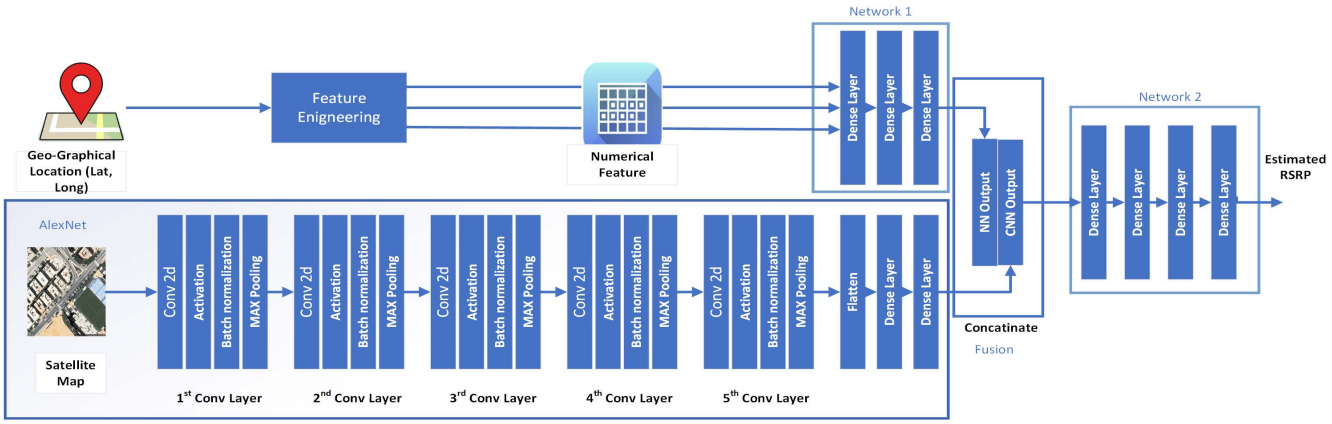

FIGURE 4. Multi-modal model architecture. Network 1 for feature extraction from the first modality, AlexNet for the environmental features extraction from the satellite images (the second modality) and Network 2 for the fusion between the two modalities.

different types of features, we use the direct LoS path between TX and RX, detect the type of objects in the direct path, or calculate the contribution of different objects in the direct path, or getting information about all the environment and obstacles around the receiver location. That is why we use a well known convolutional neural network architecture to extract the essential features that impact the output (RSRP).

5) MODEL ARCHITECTURE

This section presents the network structure. Figure 4 shows the block diagram and components of the multi-modal model. We have three main networks. The first is one of the well-known backbone networks for computer vision, the AlexNet. We are using the well-known ConvNet AlexNet architecture proposed by Alex Krizhevsky *et al.* [55]. AlexNet is one of the dominant backbone networks used in image feature extraction and won ImageNet LSVRC-2010 to classify the 1.2 million high-resolution images into the 1000 different classes. It consists of five main convolutional blocks. Each block has building layers with different convolution kernel filters, Relu activation functions, and batch normalization layer followed by flatten and dense layers. Table 2 shows the detailed configuration and parameters for the AlexNet network. We use AlexNet for image modality to extract the features that impact the RSRP value. The second network (Network 1 in figure 4) is a feed-forward neural network (FNN) to extract features from the numerical modality by adjusting neural network weights that influence the RSRP values. We use a late fusion strategy to concatenate the extracted features from networks one and two. We use a final FNN (Network 2 in Figure 4) to mix and produce a regression prediction for the RSRP value for the output of the two networks (network 1 and AlexNet). Table 3 shows detailed architecture of network 1 and network 2.

6) MODEL TRAINING

This section will explain the training process and parameters for the model. First, we have two datasets, the first in the Cairo region with 172,600 data points and the second in the Giza region with 118,995 data points. We download the corresponding image for each drive test data point using the satellite maps API presented in section III-A2. We resize the image to $160 \times 160 \times 3$ to fit the device's memory used during the training process. We use a laptop with a dedicated 4 GB GPU accelerator and 16 GB of RAM and equipped with an SSD hard disk. We build the model using the Tensorflow framework. Then, we train the model using Cairo dataset with 20% of the data used for validation. We exploit different model parameters to reach the optimum one we used. We use a batch size of 128, the learning rate is 0.001, and Adam optimizer with Root Mean Squared Error as a cost function. The ground truth is the RSRP values of the drive test data, and the input features are numerical features ($\mathcal{D}$, $\mathcal{LAT}$, $\mathcal{LONG}$, PL_{urban}, *bearing*) discussed earlier which is considered the first modality. The second modality is the satellite map image discussed above. We train the model for 10 hours to converge for the best accuracy. We use the mean absolute error as the primary metric for accuracy.

B. ONLINE MODE

The online mode dynamically estimates the RSRP values in any given location. It consists of four modules similar to the online mode, except that we have the needed location to calculate the coverage map/RSRP in module two. We download the satellite image for the needed locations using Google Maps API and combine it with cell configuration data using the geographical locations. The pre-trained model is initialized with the output weights of the offline stage. The output of the online stage is a coverage Map that shows the RSRP values in the input locations.

TABLE 2. ALexNet network architecture details.

Layer	Type	Input	Filter Size	Number of filters	Output
1st Conv Block	Conv2d	160x160x3	(11x11)	96	40x40x96
	Activation	Relu Activation			
	Batch Normalization	Batch Normalization Layer			
	Max Pooling	40x40x96	(2x2)		20x20x96
2nd Conv Block	Conv2d	20x20x96	(5x5)	256	20x20x256
	Activation	Relu Activation			
	Batch Normalization	Batch Normalization Layer			
	Max Pooling	20x20x256	(2x2)		10x10x256
3rd Conv Block	Conv2d	10x10x256	(3x3)	384	10x10x384
	Activation	Relu Activation			
	Batch Normalization	Batch Normalization Layer			
4th Conv Block	Conv2d	10x10x384	(3x3)	384	10x10x384
	Activation	Relu Activation			
	Batch Normalization	Batch Normalization Layer			
5th Conv Block	Conv2d	10x10x384	(3x3)	256	10x10x256
	Activation	Relu Activation			
	Batch Normalization	Batch Normalization Layer			
	Max Pooling	10x10x256	(2x2)		5x5x256
6th Layer	Flatten	Flatten Layer Output 6400			
7th Layer	Dense	Dense Layer with 1024 Neuron			
8th Layer	Dense	Dense Layer with 256 Neuron			

TABLE 3. Network 1 and Network 2 architecture details.

Network	Type	Number of Neurons	Activation
Network 1	Dense Layer	64	relu
	Dense Layer	64	relu
	Dense Layer	64	relu
Network 2	Dense Layer	128	relu
	Dense Layer	64	relu
	Dense Layer	32	relu
	Dense Layer	1	linear

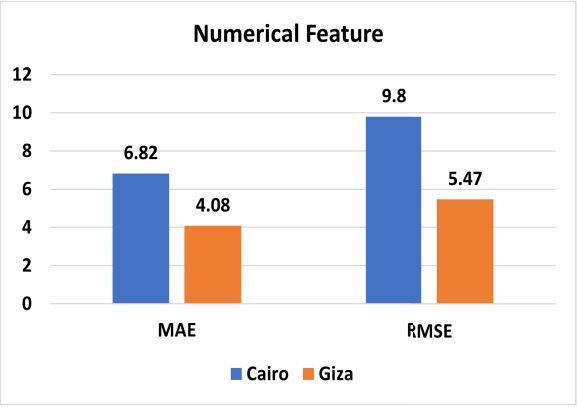

FIGURE 5. Numerical features output for Cairo and Giza dataset.

IV. PERFORMANCE EVALUATION AND DISCUSSION

In this section, we present the results of our model with different views. we use two metrics to evaluate the results, the Mean Absolute Error (MAE) defined by equation (9) and the Root Mean Square Error (RMSE) defined by equation (10)

$$\text{MAE} = \frac{\sum_{i=1}^{n} |y_i - x_i|}{n} \tag{9}$$

$$\text{RMSE} = \sqrt{\frac{\sum_{i=1}^{n} (y_i - x_i)^2}{n}} \tag{10}$$

where y_i is the predicted value and x_i is the true value.

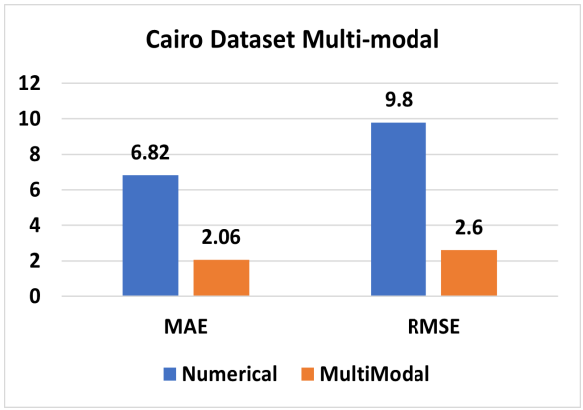

FIGURE 6. Multi modal output for Cairo region.

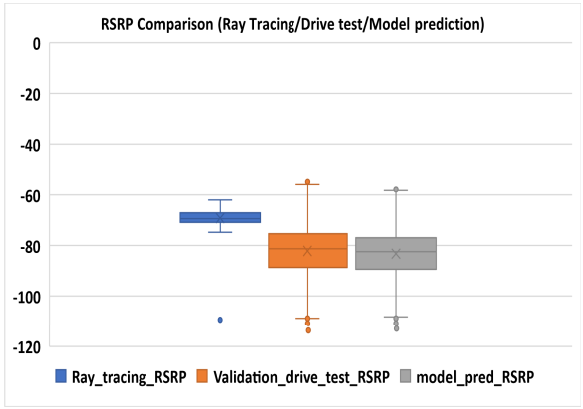

FIGURE 7. multi modal boxplot Cairo dataset.

A. NUMERICAL FEATURES ONLY

In this section, we present the result of the model based on the numerical features explained in the feature engineering section III-A4. Figure 5 shows that the MAE for Cairo dataset

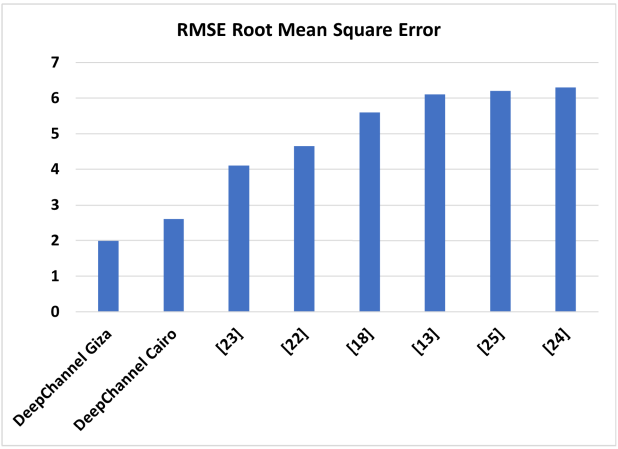

FIGURE 8. Comparison between different path loss prediction models showing the low RMSE for DeepChannel model in the Cairo area and Giza area with transfer learning.

TABLE 4. Distribution distance and measure of variability.

Parameter	Validation drive test RSRP	Model pred RSRP	Ray tracing RSRP
Mean	-83.3	-83.3	-69.1
STD	9.4	8.8	2.5
Coefficient of variation	-8.9	-9.4	-27.8

is 6.82 *dB*, and RMSE is 9.8 *dB*, while for the Giza dataset, the MAE is 4.08 *dB*, and the RMSE is 5.47 *dB*. These are relatively high values that we can not depend on in actual practical predictions. The accuracy of Giza is higher than Cairo's accuracy as the geographical characteristics in the Cairo region are denser than Giza region. Therefore, the RSRP values in Cairo region suffer from different conditions (scattering, reflection, refraction) that significantly affects the RSRP.

B. MULTI-MODAL PERFORMANCE

This section presents the multi-modal system (Figure 4) output for both datasets. Figure 6 shows the results for the Cairo dataset compared to the numerical features only. We can see that the proposed multi-modal model achieves MAE of 2.06 *dB* with 4.8 *dB* enhancement and RMSE of 2.05 *dB* with 7.8 *dB* enhancement.

We complete our study by comparing our multimodal prediction system with the drive test RSRP values and the values from the ray tracing system. Figure 7 shows a box plot for the actual values of the validation RSRP values from the driving test, the ray-tracing simulations, and the predicted RSRP values from the model. We export the ray-tracing simulation result from a third-party application provider in the same driving test area. The distributions of the driving test and multi-modal prediction are almost identical with the same interquartile range and statistical parameters, showing the proposed model's high accuracy and nearest to the drive test practical measurements. However, the ray-tracing model output is a different distribution with a small interquartile range indicating that the resultant RSRP values are within a small range and can not capture the accurate environmental features impacting the actual RSRP values.

TABLE 5. Transfer learning.

Transfer learning	MAE	RMSE	Training Time
Without	1.89	2.4	5.3 hours
With	1.47	1.99	1.2 hour

Table 4 shows the statistical parameters with the coefficient of variation between the validation drive test RSRP from field, model predicted RSRP and the ray tracing RSRP. The values of the mean and standard deviation (STD) of the validation drive test RSRP and the model predicted values are very close to each other and the coefficient of variation as well showing the similarity between the two distributions. On the other hand we have a much high difference between the validation drive test data and the ray tracing RSRP values.

Figure 9 shows the geographical plot of different RSRP values for the Cairo dataset's actual (Drive Test Data), ray tracing, and predicted values. We can see that almost all the points in the actual values and multi-modal model predicted values are the same with the same range of values in the same points, while the ray tracing values are far from the actual values. Thus, the multi-modal output accurately predicts the RSRP using satellite images to extract environmental features.

A comprehensive comparison of different path loss prediction systems are shown in figure 8. It shows that the DeepChannel multi-modal model architecture, with handcrafted features, can achieve better accuracy than the state-of-the-art techniques using deep learning only or jointly with images.

C. TRANSFER LEARNING

Transfer learning is a state-of-the-art technique to leverage the training processing and converge to the optimum weights that achieve the best predictions. Then, initialize a new network model with these weights and use them for the prediction with minor changes to fit the new dataset. This process directly saves training time and computation powers with the opportunity to achieve higher accuracy. We use the model's weights trained in area one as the initialization for area two. Table 5 shows the model accuracy for dataset two with and without transfer learning. The MAE and RMSE are enhanced with about 20.2% and, we have a 77.35% reduction in training time.

V. DISCUSSION

In the performance and evaluation section we show the robustness of DeepChannel model, and the high accuracy compared to ray tracing models and the state-of-the-art techniques. Service providers network planning and optimization

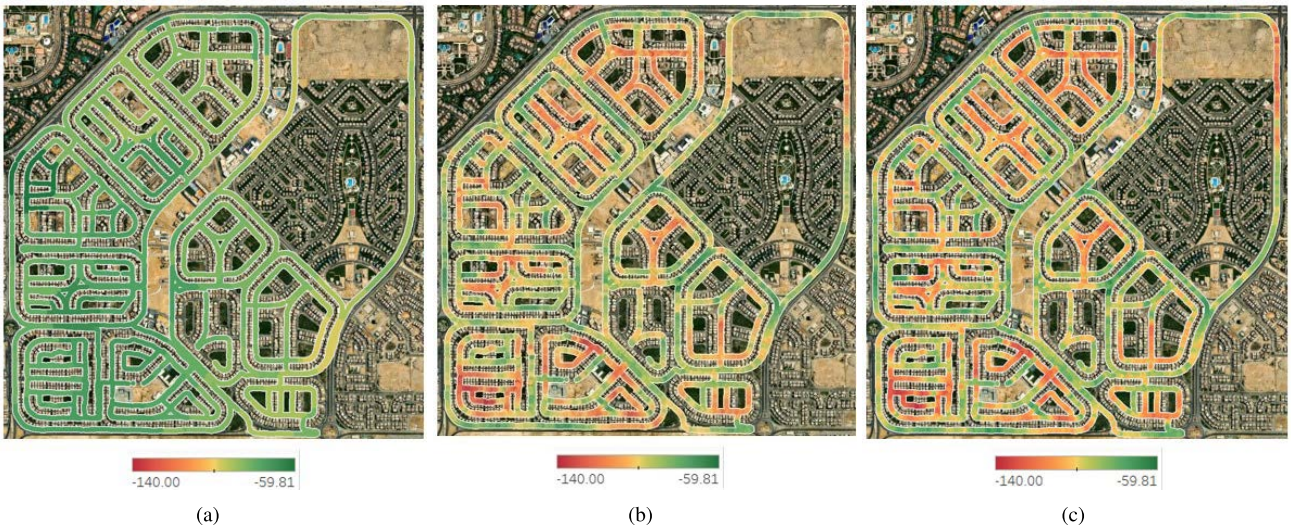

FIGURE 9. (a) Ray tracing output (b) Drive test result (c) Multimodal prediction output.

can be significantly enhanced using the DeepChannel model. In the planning phase, service providers planning engineers select the optimum location of the new base station to solve coverage problems based on ray tracing models which as shown in section IV-B is not accurate and service providers cannot rely on these data as the main input to the planning phase. The second method is to build the coverage map from drive test data with each newly deployed base station which is a very expensive and time-consuming process. Accordingly, build a trained model on different area characteristics is used to estimate the coverage map with high accuracy. Therefore, DeepChannel model is adopted with transfer learning methodology explained in section IV-C to build the coverage map taking into consideration the environmental characteristics of the area and build an accurate channel model that can be used in the planning process of selecting the optimum base station locations. The second process of service provider is to optimize the current network base station to solve customer coverage or capacity complaints related to bad experience. The optimization process comprises changing some configuration parameters to solve the subjected problem. To examine the result of the action taken in the optimization process, we should rely on the ray tracing techniques which is not accurate as explained in section IV-B or drive test data and with the nature of the optimization process from try and errors many drive test data needed after any action to examine the results. Accordingly, DeepChannel model is utilized to examine the output of the optimization process, however, the usage of DeepChannel model is limited to the parameters associated with coverage parameters. A major factor of the robustness of the DeepChannel model is we can adopt transfer learning from different areas to build a robust model. Therefore, the model must be retrained when the area characteristics is changed based on area demographic conditions and real-estate investments [56], [57].

VI. CONCLUSION

Coverage prediction plays a vital role in the daily operation of mobile service providers to enhance customer experiences and smart allocation for new investments. Thus, we have introduced DeepChannel, a multi-modal deep learning model for path loss and coverage prediction by predicting the RSRP values in 4G networks in 2100 MHz band. Our proposed architecture with the handcrafted features achieves a high prediction accuracy compared to state-of-the-art models. Using the satellite maps as a new modality with numerical features has significantly enhanced the prediction accuracy. We have tested our model with physical drive test data collected from two different areas with different characteristics. We have compared our results with the drive test data, which is a better comparison than ray tracing data which is not accurate. In addition, we have compared our model results with the ray-tracing output. The results have shown a considerable accuracy of the DeepChannel model with similar distribution to the drive test data. Moreover, we have utilized the transfer learning paradigm to transfer model weights trained in one area to another to save training computation time and power. DeepChannel uses multiple modalities to extract the environmental features that impact the path loss in 4G networks in different area characteristics. In our future work, we will use image semantic segmentation to capture the different objects from the satellite image. Finally, we can test DeepChannel in different operating frequency band and for new evolving mobile technologies such as 5G, 6G.

ACKNOWLEDGMENT

The authors would like to thank Ayman Gaber, Radio Strategy and Engineering Sr. Manager, and Mostafa Essa, AI and Data Analytics Distinguished Engineer from Vodafone, Egypt, who provided insights and expertise that greatly assisted the research.

REFERENCES

[1] C. X. Wang, J. Huang, H. Wang, X. Gao, X. You, and Y. Hao, "6G wireless channel measurements and models: Trends and challenges," *IEEE Veh. Technol. Mag.*, vol. 15, no. 4, pp. 22–32, Dec. 2020, doi: 10.1109/MVT.2020.3018436.

[2] *Evolved Universal Terrestrial Radio Access (E-UTRA); Physical layer—Measurements*, 3GPP, document TS 36.214, 2017.

[3] A. Mohamed, M. Tharwat, M. Magdy, T. Abubakr, O. Nasr, and M. Youssef, "DeepFeat: Robust large-scale multi-features outdoor localization in LTE networks using deep learning," *IEEE Access*, vol. 10, pp. 3400–3414, 2022, doi: 10.1109/ACCESS.2022.3140292.

[4] O. O. Erunkulu, A. M. Zungeru, C. K. Lebekwe, and J. M. Chuma, "Cellular communications coverage prediction techniques: A survey and comparison," *IEEE Access*, vol. 8, pp. 113052–113077, 2020, doi: 10.1109/ACCESS.2020.3003247.

[5] T. S. Rappaport and K. B. H. Xu, "Propagation and radio system design issues in mobile radio systems for the GloMo project," Virginia Polytech. Inst. State Univ., Blacksburg, VA, USA, Tech. Rep., 1997.

[6] K. Rizk, J.-F. Wagen, and F. Gardiol, "Two-dimensional ray-tracing modeling for propagation prediction in microcellular environments," *IEEE Trans. Veh. Technol.*, vol. 46, no. 2, pp. 508–518, May 1997, doi: 10.1109/25.580789.

[7] J. W. McKown and R. L. Hamilton, Jr., "Ray tracing as a design tool for radio networks," *IEEE Netw.*, vol. 5, no. 6, pp. 27–30, Nov. 1991, doi: 10.1109/65.103807.

[8] C. Phillips, D. Sicker, and D. Grunwald, "A survey of wireless path loss prediction and coverage mapping methods," *IEEE Commun. Surveys Tuts.*, vol. 15, no. 1, pp. 255–270, 1st Quart., 2013, doi: 10.1109/SURV.2012.022412.00172.

[9] K. A. Chamberlin and R. J. Luebbers, "An evaluation of Longley–Rice and GTD propagation models," *IEEE Trans. Antennas Propag.*, vol. AP-30, no. 6, pp. 1093–1098, Nov. 1982, doi: 10.1109/TAP.1982.1142958.

[10] M. I. Jordan and T. M. Mitchell, "Machine learning: Trends, perspectives, and prospects," *Science*, vol. 349, no. 6245, pp. 255–260, 2015.

[11] N. Moraitis, L. Tsipi, and D. Vouyioukas, "Machine learning-based methods for path loss prediction in urban environment for LTE networks," in *Proc. 16th Int. Conf. Wireless Mobile Comput., Netw. Commun. (WiMob)*, Oct. 2020, pp. 1–6, doi: 10.1109/WiMob50308.2020.9253369.

[12] O. Ahmadien, H. F. Ates, T. Baykas, and B. K. Gunturk, "Predicting path loss distribution of an area from satellite images using deep learning," *IEEE Access*, vol. 8, pp. 64982–64991, 2020, doi: 10.1109/ACCESS.2020.2985929.

[13] J. Thrane, B. Sliwa, C. Wietfeld, and H. L. Christiansen, "Deep learning-based signal strength prediction using geographical images and expert knowledge," in *Proc. IEEE Global Commun. Conf.*, Dec. 2020, pp. 1–6, doi: 10.1109/GLOBECOM42002.2020.9322089.

[14] E. Krijestorac, S. Hanna, and D. Cabric, "Spatial signal strength prediction using 3D maps and deep learning," in *Proc. IEEE Int. Conf. Commun.*, Jun. 2021, pp. 1–6, doi: 10.1109/ICC42927.2021.9500970.

[15] Y. Zhang, J. Wen, G. Yang, Z. He, and X. Luo, "Air-to-air path loss prediction based on machine learning methods in urban environments," *Wireless Commun. Mobile Comput.*, vol. 2018, pp. 1–9, Jun. 2018, doi: 10.1155/2018/8489326.

[16] S. P. Sotiroudis, S. K. Goudos, and K. Siakavara, "Neural networks and random forests: A comparison regarding prediction of propagation path loss for NB-IoT networks," in *Proc. 8th Int. Conf. Mod. Circuits Syst. Technol. (MOCAST)*, May 2019, pp. 1–4, doi: 10.1109/MOCAST.2019.8741751.

[17] L. Wu, D. He, B. Ai, J. Wang, H. Qi, K. Guan, and Z. Zhong, "Artificial neural network based path loss prediction for wireless communication network," *IEEE Access*, vol. 8, pp. 199523–199538, 2020, doi: 10.1109/ACCESS.2020.3035209.

[18] V. V. Ratnam, H. Chen, S. Pawar, B. Zhang, C. J. Zhang, Y.-J. Kim, S. Lee, M. Cho, and S.-R. Yoon, "FadeNet: Deep learning-based mm-wave large-scale channel fading prediction and its applications," *IEEE Access*, vol. 9, pp. 3278–3290, 2021, doi: 10.1109/ACCESS.2020.3048583.

[19] S. P. Sotiroudis, P. Sarigiannidis, S. K. Goudos, and K. Siakavara, "Fusing diverse input modalities for path loss prediction: A deep learning approach," *IEEE Access*, vol. 9, pp. 30441–30451, 2021, doi: 10.1109/ACCESS.2021.3059589.

[20] S. Phaiboon, P. Phokharatkul, and P. Kittithamavongs, "Mobile path loss prediction with image segmentation and classification," in *Proc. Int. Conf. Microw. Millim. Wave Technol.*, Apr. 2007, pp. 1–4, doi: 10.1109/ICMMT.2007.381345.

[21] L. Wu, D. He, K. Guan, B. Ai, C. Briso-Rodriguez, T. Shui, C. Liu, L. Zhu, and X. Shen, "Received power prediction for suburban environment based on neural network," in *Proc. Int. Conf. Inf. Netw. (ICOIN)*, Jan. 2020, pp. 35–39, doi: 10.1109/ICOIN48656.2020.9016532.

[22] H.-S. Jo, C. Park, E. Lee, H. K. Choi, and J. Park, "Path loss prediction based on machine learning techniques: Principal component analysis, artificial neural network, and Gaussian process," *Sensors*, vol. 20, no. 7, p. 1927, Mar. 2020, doi: 10.3390/S20071927.

[23] J. Thrane, D. Zibar, and H. L. Christiansen, "Model-aided deep learning method for path loss prediction in mobile communication systems at 2.6 GHz," *IEEE Access*, vol. 8, pp. 7925–7936, 2020, doi: 10.1109/ACCESS.2020.2964103.

[24] C. Park, D. K. Tettey, and H.-S. Jo, "Artificial neural network modeling for path loss prediction in urban environments," 2019, *arXiv:1904.02383*.

[25] U. Masood, H. Farooq, and A. Imran, "A machine learning based 3D propagation model for intelligent future cellular networks," in *Proc. IEEE Global Commun. Conf. (GLOBECOM)*, Dec. 2019, pp. 1–6, doi: 10.1109/GLOBECOM38437.2019.9014187.

[26] R.-T. Juang, "Explainable deep-learning-based path loss prediction from path profiles in urban environments," *Appl. Sci.*, vol. 11, no. 15, p. 6690, Jul. 2021, doi: 10.3390/APP11156690.

[27] E. M. Vitucci, V. Degli-Esposti, F. Fuschini, J. S. Lu, M. Barbiroli, J. N. Wu, M. Zoli, J. J. Zhu, and H. L. Bertoni, "Ray tracing RF field prediction: An unforgiving validation," *Int. J. Antennas Propag.*, vol. 2015, pp. 1–11, Aug. 2015.

[28] H. F. Ates, S. M. Hashir, T. Baykas, and B. K. Gunturk, "Path loss exponent and shadowing factor prediction from satellite images using deep learning," *IEEE Access*, vol. 7, pp. 101366–101375, 2019, doi: 10.1109/ACCESS.2019.2931072.

[29] Y. Okumura, E. Ohmori, T. Kawano, and K. Fukuda, "Field strength and its variability in VHF and UHF land-mobile radio service," *Rev. Elect. Commun. Lab.*, vol. 16, nos. 9–10, pp. 825–873, 1968.

[30] M. Hatay, "Empirical formula for propagation loss in land mobile radio services," *IEEE Trans. Veh. Technol.*, vol. VT-29, no. 3, pp. 317–325, Aug. 1980, doi: 10.1109/T-VT.1980.23859.

[31] *Digital Land Mobile Radio Communications*, Commission Eur. Communities Directorate-Gen. Telecommun. Inf. Industries Innov., Luxembourg, U.K., 1989.

[32] E. Damosso and G. D. Brito, "COST 231 achievements as a support to the development of UMTS: A look into the future," *IEEE Commun. Mag.*, vol. 34, no. 2, pp. 90–96, Feb. 1996, doi: 10.1109/35.481302.

[33] M. S. Smith and J. E. J. Dalley, "A new methodology for deriving path loss models from cellular drive test data," in *Proc. AP Conf.*, 2000.

[34] "The analysis of the coexistence of FWA cells in the 3.4–3.8 GHz band," Electron. Commun. Committee, Eur. Conf. Postal Telecommun. Admin., ECC Rep. 33, May 2003.

[35] *Basic Concepts of WCDMA Radio Access Network*, Ericsson, Stockholm, Sweden, 2001.

[36] V. Erceg, K. V. S. Hari, M. S. Smith, D. S. Baum, K. P. Sheikh, C. Tappenden, J. M. Costa, C. Bushue, A. Sarajedini, R. Schwartz, D. Branlund, T. Kaitz, and D. Trinkwon, *Channel Models for Fixed Wireless Applications*, Standard IEEE 802.16.3c-01/29r4, Broadband Wireless Working Group, 2001, pp. 1–36.

[37] D. C. Cox, R. R. Murray, and A. W. Norris, "800-MHz attenuation measured in and around suburban houses," *AT T Bell Laboratories Tech. J.*, vol. 63, no. 6, pp. 921–954, Jul. 1984.

[38] *Universal Mobile Telecommunications System (UMTS); Spatial Channel Model for Multiple Input Multiple Output (MIMO) Simulations*, 3GPP, document TR 25.996, 2011, pp. 16–18.

[39] G. A. Karagiannis and A. D. Panagopoulos, "Dynamic lognormal shadowing framework for the performance evaluation of next generation cellular systems," *Future Internet*, vol. 11, no. 5, p. 106, May 2019.

[40] S.-C. Wang, "Artificial neural network," in *Interdisciplinary Computing in Java Programming*. Boston, MA, USA: Springer, 2003, pp. 81–100.

[41] R. Hecht-Nielsen, "Theory of the backpropagation neural network," in *Neural Networks for Perception*. New York, NY, USA: Academic, 1992, pp. 65–93.

[42] Y. LeCun, L. Bottou, Y. Bengio, and P. Haffner, "Gradient-based learning applied to document recognition," *Proc. IEEE*, vol. 86, no. 11, pp. 2278–2324, Nov. 1998, doi: 10.1109/5.726791.

[43] S. Albawi, T. A. Mohammed, and S. Al-Zawi, "Understanding of a convolutional neural network," in *Proc. Int. Conf. Eng. Technol. (ICET)*, Aug. 2017, pp. 1–6, doi: 10.1109/ICEngTechnol.2017.8308186.

[44] K. O'Shea and R. Nash, "An introduction to convolutional neural networks," 2015, *arXiv:1511.08458*.

[45] J. Gu, Z. Wang, J. Kuen, L. Ma, A. Shahroudy, B. Shuai, and T. Liu, "Recent advances in convolutional neural networks," *Pattern Recognit.*, vol. 77, pp. 354–377, May 2018.
[46] X. Qiu, L. Zhang, Y. Ren, P. Suganthan, and G. Amaratunga, "Ensemble deep learning for regression and time series forecasting," in *Proc. IEEE Symp. Comput. Intell. Ensemble Learn. (CIEL)*, Dec. 2014, pp. 1–6, doi: 10.1109/CIEL.2014.7015739.
[47] D. Baumann, "Minimization of drive tests (MDT) in mobile communication networks," in *Proc. Zum Seminar Future Internet (FI) Innov. Internet Technologien Mobilkommunikation (IITM)*, vol. 9, 2014, pp. 1–7.
[48] TEMS Portfolio. *Mobile Network Optimization*. Accessed: Sep. 6, 2021. [Online]. Available: https://www.infovista.com/tems
[49] *Google Cloud Platform (GCP)*. Accessed: Jun. 12, 2021. [Online]. Available: https://cloud.google.com/
[50] J. Ngiam, A. Khosla, M. Kim, J. Nam, H. Lee, and A. Y. Ng, "Multimodal deep learning," in *Proc. ICML*, 2011, pp. 1–8.
[51] R. A. Jacobs, M. I. Jordan, S. J. Nowlan, and G. E. Hinton, "Adaptive mixtures of local experts," *Neural Comput.*, vol. 3, no. 1, pp. 79–87, Mar. 1991, doi: 10.1162/NECO.1991.3.1.79.
[52] O. Mees, A. Eitel, and W. Burgard, "Choosing smartly: Adaptive multimodal fusion for object detection in changing environments," in *Proc. IEEE/RSJ Int. Conf. Intell. Robots Syst. (IROS)*, Oct. 2016, pp. 151–156, doi: 10.1109/IROS.2016.7759048.
[53] D. Feng, C. Haase-Schütz, L. Rosenbaum, H. Hertlein, C. Glaeser, F. Timm, W. Wiesbeck, and K. Dietmayer, "Deep multi-modal object detection and semantic segmentation for autonomous driving: Datasets, methods, and challenges," *IEEE Trans. Intell. Transp. Syst.*, vol. 22, no. 3, pp. 1341–1360, Mar. 2021, doi: 10.1109/TITS.2020.2972974.
[54] C. Reid Turner, A. Fuggetta, L. Lavazza, and A. L. Wolf, "A conceptual basis for feature engineering," *J. Syst. Softw.*, vol. 49, no. 1, pp. 3–15, Dec. 1999.
[55] A. Krizhevsky, I. Sutskever, and G. E. Hinton, "ImageNet classification with deep convolutional neural networks," in *Proc. Adv. Neural Inf. Process. Syst.*, vol. 25, 2012, pp. 1–9.
[56] L. Song and J. Shen. *Evolved Cellular Network Planning and Optimization for UMTS and LTE*. Boca Raton, FL, USA: CRC Press, 2010.
[57] *Improving Carrier ROI Through Geolocalized Network Data Analysis*. Accessed: Jun. 22, 2022. [Online]. Available: https://www.huawei.com/en/technology-insights/publications/huawei-tech/75/improving-carrier-roi-through-geolocalized-network-data-analysis

MOHAMED THARWAT WAHEED graduated from the Electronics and Communication Department, Faculty of Engineering, Cairo University, in 2006. He received the M.Sc. degree in using reinforcement learning in mobile communication, in 2017. He is currently pursuing the Ph.D. degree with Cairo University in the applications of AI/ML in the Telecom industry. He is also working as a Subject Matter Expert in technology domain with Vodafone, Egypt. His research interests include the IoT in smart cities, 5G, autonomous driving, AI/ML in mobile communication, and SDN/NFV in mobile networks.

YASMINE FAHMY received the B.Sc. (Hons.), M.Sc., and Ph.D. degrees in telecommunications from the Faculty of Engineering, Cairo University, in 1999, 2001, and 2005, respectively. She is currently a Professor at the Electronics and Communications Department, Faculty of Engineering, Cairo University. She led and participated in many research projects with a vision of linking the telecommunication industry to the academia in Egypt and have a distinguished record of publication in internationally recognized journals. Her current research interests include wireless communications, modern coding techniques, and MIMO systems.

AHMED KHATTAB (Senior Member, IEEE) was born in Cairo, Egypt, in 1980. He received the B.Sc. (Hons.) and M.Sc. degrees in electrical engineering from Cairo University, Cairo, in 2002 and 2004, respectively, the Master of Electrical Engineering degree from Rice University, in 2009, and the Ph.D. degree in computer engineering from the Center for Advanced Computer Studies (CACS), University of Louisiana at Lafayette, in 2011. He is currently an Associate Professor with the Electronics and Electrical Communications Engineering Department, Cairo University, where he joined as an Assistant Professor, in 2012. He authored/coauthored three books, four book chapters, over 100 journal and conference publications, and a U.S. patent. His current research interests include wireless networking, including the Internet of Things (IoT), wireless sensor networks, vehicular networks, cognitive radio networks, security, and machine learning. He received the Cairo University Excellence Award for Advanced Technological Sciences in 2021. He was a recipient of the Egypt State First Class Medallion of Excellence in 2019, the Egypt State Encouragement Award for Engineering Sciences in 2017, and the Cairo University Excellence Award in Advanced Technology Sciences in 2020. He has also won several awards from different IEEE conferences and societies.